Final Report

for NASA Grant NAG-1-1443

Optical Fiber Spectroscopy

Submitted by

A. M. Buoncristiani

**Department of Physics,
Computer Science and Engineering**

Christopher Newport University

October 25, 1999

Introduction

This is the final report of work done on NASA Grant NAG-1-1443. The work covers the period from July 1, 1992 to December 1, 1998. During this period several distinct but related research studies and work tasks were undertaken. These different subjects are enumerated below with a description of the work done on each of them. The focus of the research was the development of optical fibers for use as distributed temperature and stress sensors. The initial concept was to utilize the utilize the temperature and stress dependence of emission from rare earth and transition metal ions substitutionally doped into crystalline or glass fibers. During the course of investigating this it became clear that fiber Bragg gratings provided a alternative for making the desired measurements and there was a shift of research focus on to include the photo-refractive properties of germano-silicate glasses used for most gratings and to the possibility of developing fiber laser sources for an integrated optical sensor in the research effort.

During the course of this work several students from Christopher Newport University and other universities participated in this effort. Their names are listed below. Their participation was an important part of their education.

List of Students Who Participated in NAG-1-1443

Graduate Students
Arnel Lavarias, (MS and PhD, Old Dominion University)
Alvin Bryant, (MS, Old Dominion University)
Paul Malas (MS from Christopher Newport University)
John Michael Hall (Masters student from Christopher Newport University)

Undergraduate Students
Jay Chabo (BS, Christopher Newport University)
Brian Drumond, (Christopher Newport University transfer student)
Brian Maddox (BS, Longwood College)
Kim Haddock (BS, Christopher Newport University)
Monica Oliveras-Valentin (BEE, University of Puerto Rico)

Description of the work

1) Optical fiber spectroscopy (1992-1994).

The effects of local environmental characteristics such as stress and temperature on the optical properties of the transition metal and lanthanide rare earth ions substitutionally doped into crystalline and glass hosts has been extensively studied and are now well understood. A new technique, laser heated pedestal growth, allows the fabrication of crystalline fibers to be fabricated. These fibers display the same optical properties in the fibers as they do in bulk material. The focus of this work was to explore the possibility of using these properties in an optical fiber sensor. Most of the work dealt with examination of the properties of the Europium ion doped into Y_2O_3 and modeling these characteristics for use in a sensor.

The Y_2O_3 crystal has a cubic structure with unit cell dimension 10.61 Å. Each yttrium ion has six oxygen ions as nearest neighbors configured to occupy six of the eight corners of a cube surrounding the yttrium ion. There are two distinct arrangements of the oxygen around each yttrium site. In one arrangement the two vacant oxygen sites are at opposite

diagonals of the cube forming a high symmetry (centro-symmetric) site of symmetry C3i ; in the other arrangement the oxygen vacancies are at opposite diagonals of a cube face forming a low symmetry site of symmetry Cs. The triply ionized Europium ion is in a $_4f^6$ electron configuration and substitutes for the triply ionized Yttrium ion in either of these two distinct crystallographic sites. There are three of the low symmetry Cs sites for each C3i site. A Europium ion at a Cs site will have its degeneracy fully broken but it will be only partially broken in the C3i site. The energy levels and Stark splittings for Eu $^{3+}$:Y_2O_3 are well known and correspond to theoretical predictions.

The radiative transitions between the between $_5D^2$ -->$_7F^6$ manifolds are strongly quenched above room temperature so they would not be expected to contribute the high temperature luminescence; this has been demonstrated by Klassen. On the other hand one can expect contributions from both of the Stark level transitions connecting the $_5D^0$ -->$_7F^2$ manifolds. For the CS symmetry sites, there are three major Stark levels in the $_7F^2$ manifold and one in the $_5D^0$ manifold; these contribute to emission at 611.36, 613.12 and 631.4 nm. As shown in sequel, the asymmetry observed in the spectral shape of the emission near 611 nm line is due to the combined emission from the nearby transitions at 611.36 and 613.12 nm. There may be additional contributions to this lineshape from phonon sidebands, however these are not expected to be large since the vibronic coupling to the Y_2O_3 lattice has been shown to be weak both theoretically and experimentally.
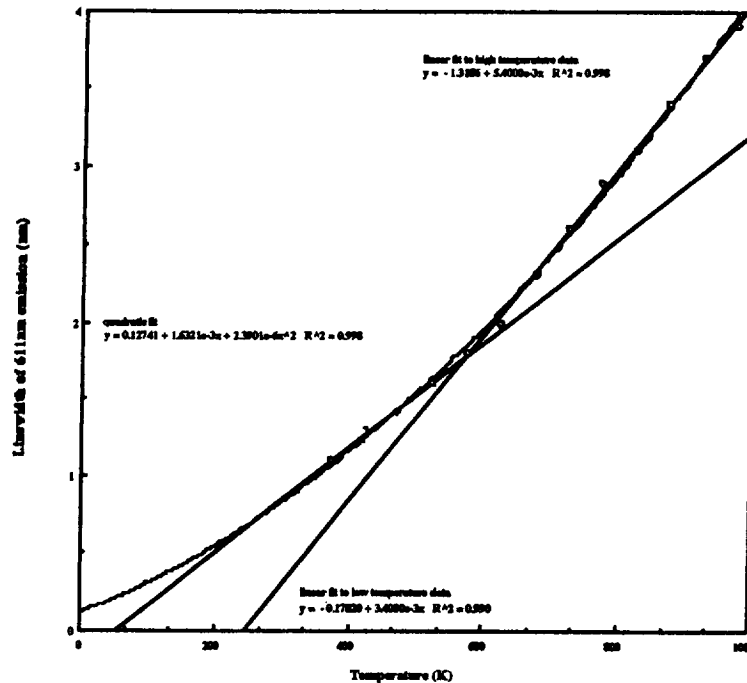*

Figure 1. Measured values of the linewidth of the 611 nm emission of Eu $^{3+}$: Y_2O_3 from Albin. Curves indicate a quadratic fit to the data and linear regression fitting to the low and high temperature regions separately.

Albin and his students at Old Dominion University have measured the emission spectra of $Eu^{3+} : Y_2O_3$ in the region of 611nm at temperatures ranging from 323 K to 973 K. These measurements were made on powdered samples thermally diffused into an optical fiber which was used to collect the emitted light. The temperature dependence of the linewidth extracted from these spectra is shown in Figure 1. The raw data is fit to a quadratic expression in temperature. In the following we develop a model for this temperature dependence.
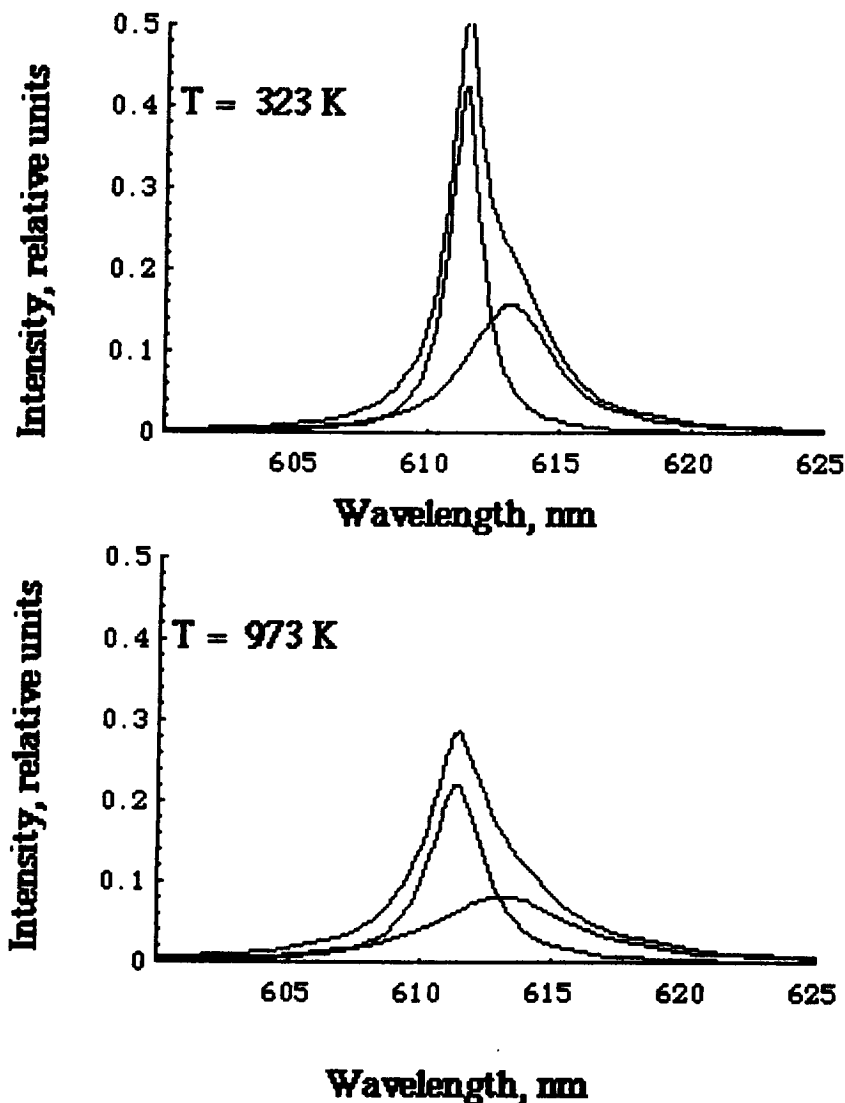

Figure 2. The calculated lineshape for the 611 nm emission assuming that two nearby Stark level transitions (611.36 nm and 613.12 nm) contribute. Each level has a Lorentz lineshape which changes with temperature according to the Frank-Condon factor.

The previous calculations assumed that a single phonon energy Ep was available to broaden the electronic transitions but that many of these phonons of this energy could participate in the transition. We now consider a process involving a single phonon of energy $h\omega$ to calculate the temperature dependence of the linewidth of the 611.4 nm emission. We can fit the measured linewidth using a model of the electron-phonon interaction involving single phonon processes. From McCumber and Sturge the single phonon contribution to linewidth has the form

$$\Delta v_{phonon} = \frac{|C_{12}|^2}{2\pi} \frac{V}{v^5} \omega^3 \left(e^{\bar{h}\omega/kT} - 1 \right)^{-1},$$

where C_{12} is the matrix element for the transition and gives the strength of the electron-phonon coupling, V is the volume of the crystal, v is its speed of sound (assuming the transverse and longitudinal speeds are equal), and $h\omega$ is the single phonon energy.

The data taken by Albin can be fit to the following expression,

$$\Delta v = a + b \, \omega 3 \, (exp(h\omega/kT) - 1)-1 . \tag{8}$$

with a = 0.0434, b = 0.0000135 and Ep = $h\omega$ = 68.7 meV (554 cm-1). The single phonon energy is within the phonon spectrum for this host and is in fact close to the value found in Reference 11 for the phonon responsible for quenching the 5DJ manifolds. This fit is very good.

In addition to this study based on the Europium ion there were also parallel studies on the optical properties of Sapphire crystalline fibers. The absorption and emission spectra of sapphire fibers were measured at several temperatures. A new technique was developed for determining the scattering from the fibers using an integrating sphere.

2) Studies of Thermal damage in Cable insulation (1995).

The following task was carried out to transfer technological on optical fiber sensors to the nuclear power industry. It was part of an exchange of information between NASA and the Idaho Nuclear Energy Laboratory. Electrical cables are an important element of the instrumentation and control in nuclear power plants. They are critical to plant safety during normal operations as well as during an unforeseen event. Much of this cabling is located inside of the containment and so is exposed to a severe environment. The cable system must function for many years under the normal, but severe, operating conditions and remain functional during and after the imposition of an abnormal condition.

A major concern about electrical systems is the loss of the mechanical and electrical integrity of the insulation on individual cables as they age. That is, the cable insulation may loose elasticity and become brittle or insulation resistance may be reduced, increasing the direct current leakage and alternating current losses. The thermal and radiation environment, especially in the presence of oxygen, is the principal cause of stress to the mechanical and electrical integrity of the polymer-based compounds that make up the cable insulation and jacket material.

In-service measurements to monitor the status of cables would be a valuable asset to the safety program of a nuclear power plant. Cable layouts are not easily accessible for

inspection because of the complexity of their layout or because of their environment. Alternative monitoring schemes, such as removing cables from service for inspection, or additional accelerated age conditioning, or direct testing for design basis event conditions are relatively expensive.

No in situ electrical testing of insulation and jacket material has been successful in detecting gradual changes due to aging. The Electrical Circuit Characterization and Diagnostic (ECCAD) System is effective identifying and locating circuit discontinuities but it is not effective in monitoring the state of aging of the insulation and jacket material. Among alternative test and monitoring concepts are those which involve optical frequencies, especially techniques which use optical fibers in a distributed test situation.

The basic idea behind this work is to examine the possibility that changes in cable insulation and jacket material, induced by the thermal and radiation environment in nuclear power plants, can be monitored with optical fibers. We set out to identify and characterize optical changes in cable insulation due to accelerated thermal aging. Since the typical cable insulation materials are not transparent at optical frequencies we must use the optical characteristics of the surface and near surface interface. Two experimental tools are available for this study 1) ellipsometry, which measures specular reflection and 2) reflectometry, which measures diffuse reflection. We set out first to identify and characterize optical changes in cable insulation due to accelerated thermal aging. Cables obtained from INEL were thermally aged at the NASA Langley Research Center to nominal service terms of 0, 20, 40 and 60 years and analyzed at the Laser Photonics Laboratory at Christopher Newport University. We measured the specular and the diffuse components of the reflection arising from surface and sub-surface scattering centers in the cable insulation at several wavelengths in the visible and near IR regions of the spectrum. The specular reflection was measured by ellipsometry and the diffuse reflection was measured using an integrating sphere.

Because the cable insulation available to us was textured by the impression of the stranded cable which it surrounded measurements of the specular reflection were difficult to make. As a result we are not able to draw a conclusion about the influence of thermal aging on reflection from ellipsometric measurements of the specular reflection. This null result does not negate the sensor concept under investigation.

The diffuse reflectivity measurements show small changes in reflection with aging for some samples. However, for one sample there was a large change in reflectivity with accelerated aging.

While some of the measurements led to disappointing results, others offered clear evidence that changes in the cable insulation material could be monitored by optical fibers. This concept suggests that to in-service monitoring of cables in nuclear power plants may be possible.

In addition, in the course of carrying out these measurements we were able to observe some of the mechanical changes in the cable insulation resulting from accelerated thermal aging. This suggested a new concept for monitoring changes in the cable insulation. If an optical fiber were insulated by the cable material in such a way that the insulation and the fiber were bonded together, then any mechanical stress induced in the insulation by aging would be transmitted to the optical fiber. These mechanical stresses in the fiber could be detected as changes in the refractive index of the fiber.

3) Cryogenic Measurements (1996-1997).

In order to study the behavior of various sensors including Bragg gratings I designed and constructed a high vacuum, cryostat at LaRC. The design incorporated an existing vacuum system, which I had to rehabilitate. The cryostat was tested and calibrated. A variety of different measurements and tests were made with it. The following list is typical of the measurements I made with it. It is still in service today.

A pair of temperature sensors obtained for the Photonetics Corporation was tested. The Lockheed Martin Corporation was considering use of this type of interferometric (Fabry-Perot cavity) sensor for use on the cryogenic hydrogen tanks on the X-33. They had never been operated a low temperature before. Results of these tests were communicated to both of those companies. Communications with Photonetics allowed them to improve the design of their sensors .

A series of experiments over several months studied the transmission of laser light through optical fibers at low temperatures. A set of coils were fabricated from 4 meter lengths of optical fiber and held in place with a variety of experimental low temperature epoxies under consideration by Lockheed Martin. These results were also transmitted to the Lockheed-Martin Company.

A third series of experiments involved study of the transmission of IR radiation through optical fibers impregnated with Hydrogen. Briefly, Corguide SMF 21 fibers were maintained in a pressure vessel at 1500 psi of hydrogen for about 100 hours. Light from an LED (1320 nm) was passed through the hydrogen loaded fiber and monitored for about 100 hours after withdrawing the fiber from the pressure vessel. As the hydrogen diffused from the fiber core the transmission of light increased, returning after about 100 hours to 90% of its pre-loading value. These results were shared with the Lockheed Martin Company. A typical hydrogen diffusion curve is shown in the figure below.

In the course of making these measurements a number of calibrations had to be done and monitored repeatedly. Two important calibrations were made on a Hewlett- Packard spectrum analyzer and on a New Focus tunable laser.

**Transmission (at 1320 nm)
through Hydrogen Loaded SMF 21
with Elapsed Time**

$$0.79 + 0.11 \tanh [0.05 (t - 50)]$$
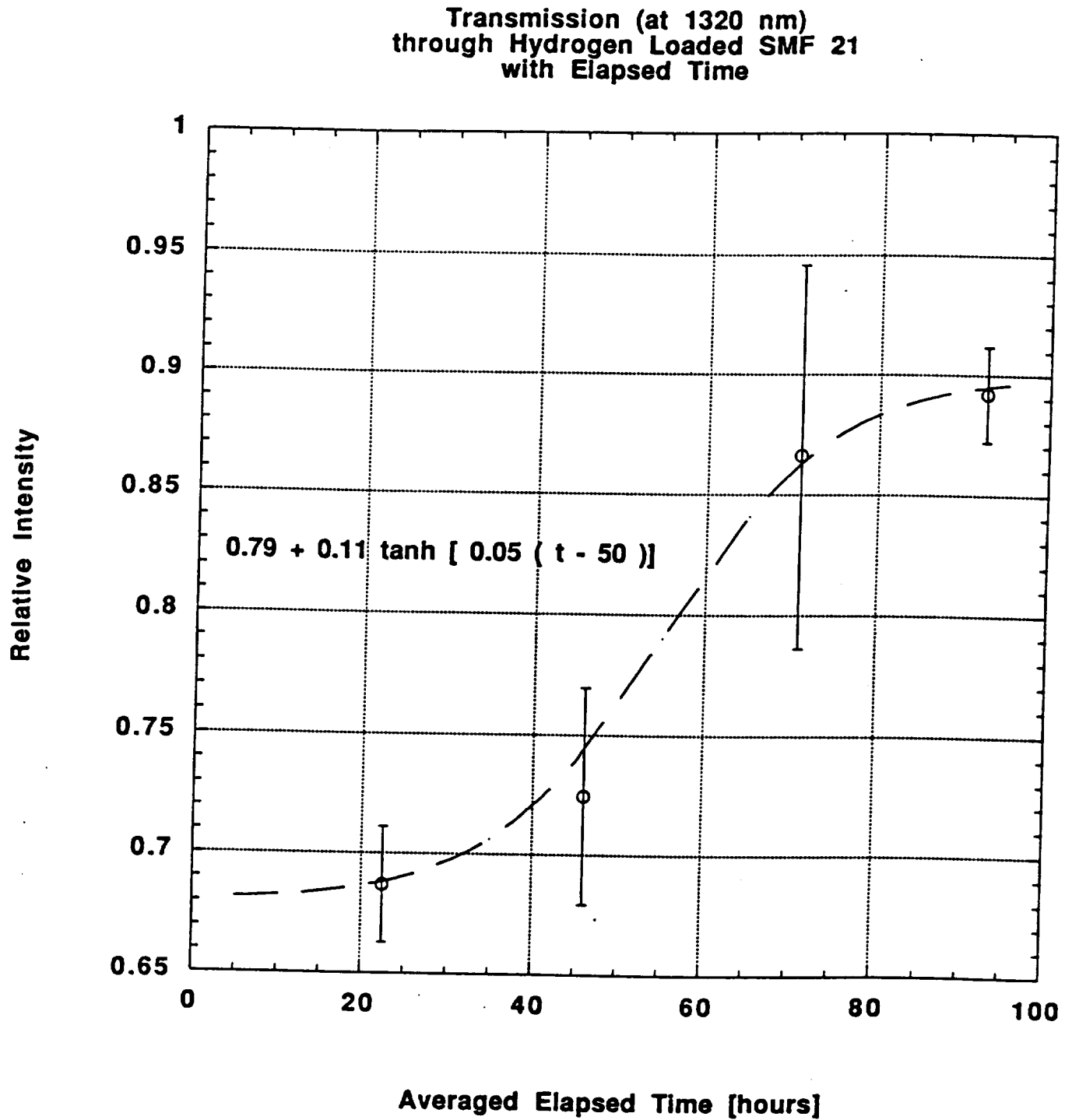
A typical IR transmission history of a hydrogen loaded fiber.

4) Bragg grating and optical fiber laser modeling (1195-1998).

Continuously tunable laser oscillators in rare earth ion doped, single mode silica fibers have become important tools for active optical fiber sensors. Successful utilization of these lasers in precision sensors requires an accurate understanding of their behavior and an important part of this understanding centers on reliable modeling. We have developed two different elements of modeling fiber laser oscillators. One element is an algorithm for the exact calculation of the reflection from a fiber Bragg grating. The second element is the introduction of a new technique for modeling the transport of radiation in a fiber with continuously changing refractive index. Using this method we are able to generate the time evolution of the distribution of radiation in a Bragg grating. This can be applied to the two major configurations of a laser oscillator -- with the active medium between two Bragg reflectors as a Fabry-Perot cavity or with the active medium overlapping the reflector region so that the optical feedback is distributed.

Research in optical fiber lasers has been dominated by the needs of the communications industry for high capacity transmission and has focused on amplifiers at the 1300 and 1550 nm fiber transmission windows. The active ions in these lasers have been trivalent rare earth ions doped into single mode silica fibers. The first rare earth doped glass lasers were studied in the early 1960's and the first rare earth fiber laser was constructed in 1987. Fiber amplifiers at 1550 nm (Erbium) and at 1310 nm (Neodymium) are now very well characterized. Recently attention has turned to the use of tunable optical fiber laser oscillators for use in active optical fiber sensors; here there is a need for a precisely tunable fiber laser oscillator. In order to develop this precise tuning it is necessary to have a detailed understanding of the optical characteristics of the fiber laser components.

UV radiation induces defects in silica-germanate fibers (Ge color centers) which result in a permanent change in the refractive index. If this photo-induced change in refraction is caused by an interference pattern of the UV light, it generates a periodic modulation of the refractive index and this is the basis for the fabrication of Bragg grating reflectors. The reflection spectrum of the Bragg gratings can be modeled using a coupled mode equation for the forward and backward propagating waves. After some restrictive approximations are made these coupled wave equations can be solved in closed form as was done by Lam and Garside.

Reflection from a Bragg reflector depends upon the normal refractive index of the fiber core, n, the spatial period of the grating, Λ, the length of the grating, L_g, the resonant wavelength of the grating, λ_B, the wavelength of propagating light, λ, and the coupling between the propagating light and the index variation, Ω. The Bragg grating resonance condition is given by

$$\lambda_B = 2 n \Lambda. \tag{1}$$

The reflection coefficient depends upon the resonance detuning.

The approximations used by Lam and Garside to obtain a system of equations that have a closed form solution are severe. We have developed rigorous and exact method for calculating the reflection and transmission coefficients for linearly polarized electric fields passing through a Bragg grating in an optical fiber. This method involves finding a numerical solution to the exact coupled mode equations over a single spatial period of the grating and then, using a recursion formula which we have developed, to extend the numerical solution over the N periods of the grating. At resonance the numerical solutions depend upon a single parameter (the coupling constant which is proportional to the depth of

modulation of the grating). Graphs of the amplitude and phase of the reflection coefficients are shown in Figures 1 and 2.
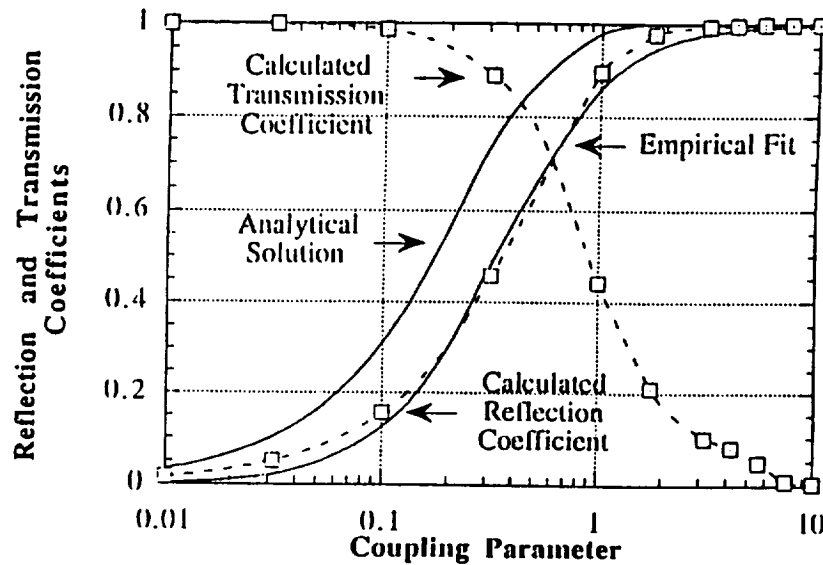

Figure 1. Magnitude of the amplitude of the reflection and transmission   coefficient as a function of coupling constant at resonance.
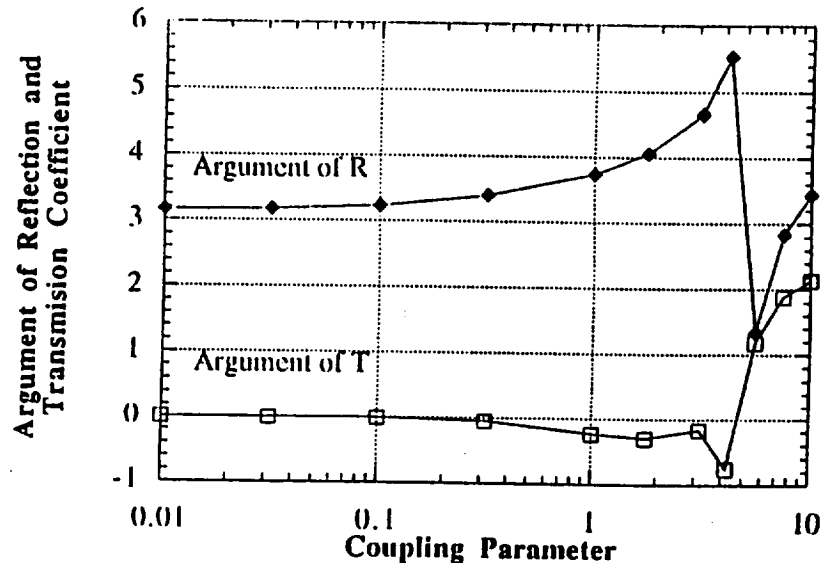

Figure 2. Argument of the reflection and transmission coefficient as a function of coupling constant at resonance.

The advantage of using this method is that it allows the numerical solution over the single period to be constructed as precisely as required for reliable results, without being constrained by the long length of the grating itself. The reason this method works for the case of a passive grating is that the reflection and transmission coefficients are identical for each spatial period and this allows treatment of the grating as a sequence of single periods. These calculations show that the solutions of Lam and Garside are good for the regions with very strong or very weak coupling. In the region where there is intermediate coupling there a significant difference between the approximate Lam and Garside solution and the exact one we have developed. There are several ways that this method can be extended. It can be used to model gratings which have partial periods by solving the appropriate

coupled wave equation over partial periods. The effects of absorption can be included rather easily by changing the constraint on the single period reflection and transmission coefficients to include the effect of absorption over the period.

There are two kinds of laser configurations, the Fabry-Perot and a distributed feedback laser where the active region is the entire Bragg grating. Typically the pumping configuration is end pumping with semiconductor diode lasers. The simplest model of laser oscillator operation is a rate equation mode in which a spatial average over the distribution of electronic energy level populations and photon concentration is taken. This sort of model works well in solid state lasers with relatively short gain lengths [8, 9] but in fiber lasers where the gain length can be large and the distribution of population over space varied, it is less appropriate. This type of model is well discussed in the literature [10-12]. If the laser cavity is L_{cavity} the laser resonance condition is given by

$$\lambda_0 = \frac{2}{m} n L_{cavity}$$

(2)

with m the mode number.

We describe a new approach to the coupled wave equations for treating light propagating in one dimension through a region of changing refractive index. The method was developed to analyze some problems associated with propagation in optical fibers with index modulation along the fiber axis, but it is applicable in other situations. The principle advantage of the method is that it allows the simultaneous treatment of propagation in both directions and includes the interaction of both propagation directions with the medium. In addition, it is easily adaptable to numerical computation. The key idea in this method is to monitor changes in the flux of the electric field traveling in both directions.

We examine the effect that local changes in refractive index have on propagating fields by considering a plane, monochromatic electromagnetic wave normally incident on a step discontinuity. If the step barrier has a width Δx, then the change in index of refraction can be written as

$$n' = n + \frac{\partial n}{\partial x} \Delta x ,$$

(3)

and the local transmission and reflection coefficients take on the form

$$t_{\pm} = 1 - \frac{1}{2n} \frac{\partial n}{\partial x} \Delta x \qquad r_{\pm} = - \frac{1}{2n} \frac{\partial n}{\partial x} \Delta x .$$

(4)

It is apparent that the local transmission and reflection factors depend on the change in refractive index encountered by the propagating wave and consequently propagation is not the same for the two directed waves passing through a region. Furthermore, the four transmission and reflection factors satisfy the following relations

$$t_+ t_- - r_+ r_- = 1$$
$$r_+ + r_- = 0$$
$$\frac{1}{2}(t_+ + t_-) = 1$$

(5)

The first two relations insure that the bi-directional reflection and transmission are invariant under time reversal of all fields. If the four factors are arranged in a matrix the first and last conditions above imply that the two matrix invariants are constant, that is independent of changes in the index.

Now consider how the field flux changes as it moves through an infinitesimal element of its path. Two functions of position and time describe the instantaneous distribution of electric fields in time; $I_+(z, t)$ and $I_-(z, t)$ give the right and left traveling fields respectively. These functions are defined for over the region $\{0 < z < L; \ t > 0\}$. An arbitrary infinitesimal element of the path sees two flux components incident upon it, one from each direction and similarly two flux components emerge from the element, one in each direction as shown in the figure below.
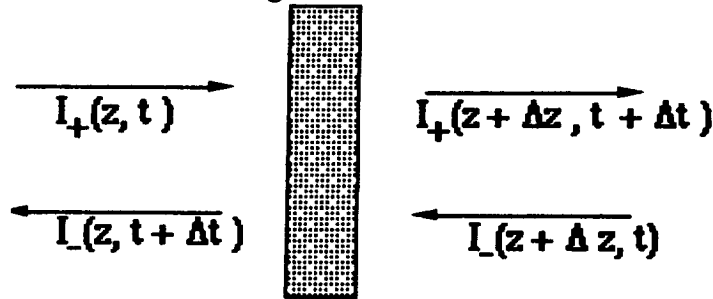

Figure 3 The relationship between field flux incident on an infinitesimal   element of the fiber and the two emergent field fluxes.

The two emerging flux components are linearly related to the two incident components by the following relations,

$$I_+(z + \Delta z, t + \Delta t) = t_+ \ I_+(z, t) \ + \ r_- I_-(z + \Delta z, t)$$
$$I_-(z, t + \Delta t) \ = t_- \ I_-(z + \Delta z, t) \ + \ r_+ I_+(z, t) \quad (6)$$

These equations account for the alteration of the electric field as it passes through an infinitesimal element, assuming only that the effects are linear and that the usual boundary conditions are satisfied. Expanding each flux term in Eq. (6) to lowest order in Δz we obtain the following partial differential equations

$$\frac{\partial I_+}{\partial z} + \frac{n}{c} \frac{\partial I_+}{\partial t} = \left(-\frac{1}{2n} \frac{\partial n}{\partial z} - \frac{\alpha}{2} \right) I_+ \ + \ \frac{1}{2n} \frac{\partial n}{\partial z} I_-$$
$$-\frac{\partial I_-}{\partial z} + \frac{n}{c} \frac{\partial I_-}{\partial t} = -\frac{1}{2n} \frac{\partial n}{\partial z} I_+ \ + \ \left(\frac{1}{2n} \frac{\partial n}{\partial z} - \frac{\alpha}{2} \right) I_- \quad (7)$$

These equations are fully equivalent to Maxwell's equations for the propagation of linearly polarized light in one dimension, through a region which does not alter the polarization. Changes in polarization could be taken into account by extending the transmission and reflection coefficients to matrices which specify how the polarization changes, but this will not be done here.

Equations (7) is a system of coupled, first order partial differential equations describing bi-directional propagation in one spatial dimension. In general, the boundary conditions should specify the initial spatial distribution of fields, $I_+(z,0)$ and $I_-(z,0)$, and the time dependent field flux incident on each spatial boundary, $I_+(0,t)$ and $I_-(L,t)$. The first step in obtaining a formal solution to these equation involves determining the characteristic curves for the system. This is accomplished by recognizing that the characteristic curves are worldlines and transforming to a new variables: $u_\pm = z - (\pm c/n) t$,

$$i_+(u_-) = I_+(z,t) \qquad i_-(u_+) = I_-(z,t) \quad (8)$$

Suppose that the propagating waves are monochromatic an so can be represented by

$$i_\pm(u_\mp) = A_\pm(u_\mp) e^{-iku_\pm}. \quad (10)$$

and then we have the coupled mode equations,

$$\frac{\partial A_+}{\partial u_-} = -\left(ik + \frac{N}{2} + \frac{\alpha}{4}\right) A_+ + \frac{N}{2} e^{i\, k(u_+ - u_-)} A_-$$

$$\frac{\partial A_-}{\partial u_+} = -\left(ik + \frac{N}{2} + \frac{\alpha}{4}\right) A_- + \frac{N}{2} e^{i\, k(u_- - u_+)} A_+$$

(11)

It is a simple matter to write the above equations as difference equations and to develop an algorithm to follow the bi-directional propagation of waves with time. We have done this and made movies of the propagation pattern. We show here a representation of the local intensity distribution achieved after a long period if evolution in Figure 4. The length of the fiber modeled is one spatial period.
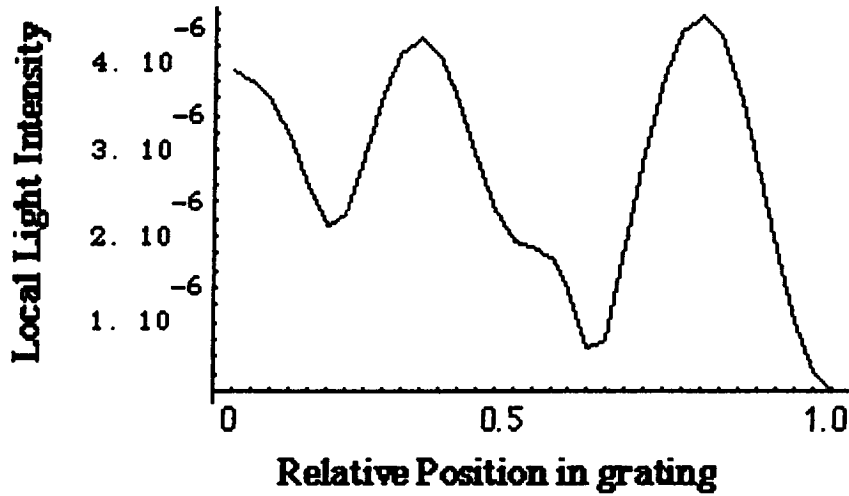

Figure 4. Distribution of steady state light intensity, under steady illumination in a single period Bragg grating.

Publications and Presentations

The following publications resulted from this work:

A.M.Buoncristiani, R.S.Rogowski, and W.M.Yen, "Activated Crystalline Fibers for Sensors, Fiber optic Sensor Based Smart Structures", Inst. Of Physics Publishing, Ltd. Bristol Eng pp. 13-17 (1992).

T.G.Wangler, J.J.Swetits and A.M.Buoncristiani, Mathl. Comput. Modelling, Vol. 17, No. 6, pp. 67-82 (1993).

A.Bryant, S.Albin, A.M.Buoncristiani, and R.S.Rogowski, "Luminescence of Eu 3+ :Y2O3 Powder Thermally Diffused into an Optical Fiber for Distributed Thermal Sensing", Optical Society of America, Vol. 19, pp.82-87. (1994).

A.M.Buoncristiani, G.Armagn, and A.A.Kaminski, "Computer Modeling of non-linearities", In Non-Linear Spectroscopy of Solids, ed. B.DiBartolo pp. 561-570. Plemum Press, New Your (1994).

S.Albin, A.C.Lavarias, J.B.Cooper, and A.M.Buoncristiani, "Thermal Effects on the Optical Properties of Eu 3+ for a Fiber Optic Temperature Sensor", Recent Res. in Optical Engineering, Vol. 1 pp. 37-56.(1996).

C.O.Egalon, A.M.Buoncristiani and R.S.Rogowski, "Asymptotic approximation and First Order Correction of the Coupled Mode Equation", Optical Engineering, Vol. 37, No. 7, pp.1930-34 (1997).

C.O.Egalon, A.M.Buoncristiani, R.S.Rogowski, A.C.Lavarias and S.Albin, Analysis of Fiber Optic Bragg Gratings, to be submitted to Optical Engineering.